

# Parametric Optimization of Pulse TIG Welding Process during Joining of Dissimilar Tensile Steels Used in Automotive Industries

A.Sahoo<sup>1, a</sup>, S. Tripathy<sup>2, b\*</sup>, D.K. Tripathy<sup>3, c</sup>

<sup>1</sup>Department of Mechanical Engineering, Institute of Technical Education and Research, Siksha 'O' Anusandhan (Deemed to be University), Bhubaneswar, India

<sup>2</sup>Department of Mechanical Engineering, Institute of Technical Education and Research, Siksha 'O' Anusandhan (Deemed to be University), Bhubaneswar, India

<sup>3</sup>Ex-Professor Emeritus, IIT Kharagpur, India

Received 8 Apr 2022

Accepted 23 Oct 2022

## Abstract

The present study focuses on multi-criteria optimization of pulse current tungsten inert gas (TIG) welding process parameters using technique for order of preference by similarity to ideal solution (TOPSIS) based Taguchi approach to enhance quality and productivity characteristics. The tig welding process is controlled by the input parameters, and optimization of process parameters is, therefore, useful for metallurgical advancements, which improve weld quality and enhance weld life. The work material used for the investigation are SAILMA 450 and EN 14B which find huge application in manufacture of rear axle in high-tech automobile industries. These materials have not been given much attention in the past but find a range of applications and hence need to be investigated. Taguchi's L<sub>25</sub> experimental design is used to investigate the influence of process parameters like peak current ( $I_p$ ), base current ( $I_b$ ), pulse frequency (F) and shielding gas flow rate (Q) on properties like yield strength (YS), ultimate tensile strength (UTS), flexural strength (FS) and microhardness (H) of the welded joints. The tensile property testing and characterization of welded sub-surface has been done to improve the weld quality and investigate the effect of welding phenomena on tensile steels. To understand the impact of pulse tig welding process parameters, analysis of variance has been used. Confirmatory tests show an improvement of 0.5457 in the preference values. The recommended settings of process parameters is found to be  $I_p=220A$ ,  $I_b =120A$ ,  $F=5Hz$  and  $Q=17l/min$ . Microstructure analysis of optimal sample shows absence of welding defects and crack formation in the fusion zone.

© 2022 Jordan Journal of Mechanical and Industrial Engineering. All rights reserved

**Keywords:** SAILMA 450, EN 14B, rear axle, pulse tig, Taguchi, TOPSIS.

## 1. Introduction

The modern manufacturing market is driven by performance quality and customer satisfaction. To obtain permanent joints and for repairing of metal components in various industries, such as manufacturing, aviation, automobile, shipbuilding, construction, power, petroleum etc., arc welding has found enormous application. Arc welding possesses advantages, such as low set up cost, ease of operation, and adaptability which make them the most sought after operations. The structural integrity and weld quality are the key measures for welding process analysis. The weld life is governed by the critical structural and material phase properties. TIG welding is among the most preferable arc welding processes because of its high precision, suitability for joining of active alloys like aluminium, magnesium, titanium and other high strength steels in different combinations due to low sensitivity to hot cracking [1,2]. The process has certain limitations like

constant heat input and wider arc formation which reduces the efficiency of the process. These drawbacks may be mitigated by gaining control over heat input which is possible with pulse current tig welding, a modified version of the traditional constant current TIG welding. In pulse current tig welding, coalescence is produced after the job gets heated by an electric arc generated between the tungsten electrode and the base metal. There is no involvement of flux and the molten metal and arc are shielded by an inert gas of either argon, helium or mixture of argon and helium. Welding current is supplied to the base material in pulses as on-time which avoids the overheating of the weld metal. Two forms of current are used as peak current and base current. Peak current is given as input to the weld metal with some time interval for melting of the base metal. The base current helps to maintain the arc ionization and allows the weld metal to cool. SAILMA 450 and EN 14B steels are commonly used for rear axle automotive parts. SAILMA 450 is widely used for machine building, lifting equipment, architectural

\* Corresponding author e-mail: sasmeetatripathy@soa.ac.in.

structures, containers, transport vehicle equipment, frame work structures, and bridge construction, and EN 14B steel is used for manufacturing machine tools, parts of the ship industry, vehicles, turbine fasteners, boiler support rods, gear shafts, valve and connecting rods, rotator blades, and excavator bucket teeth, among other applications. The joints of SAILMA 450 and EN 14B are used to make rear axles in automobile industries. The joining of dissimilar metals has always gained the attention of researchers due to the application oriented performance characteristics. Joining of dissimilar materials still remains a challenge due to property variations, and defective joining may lead to catastrophic consequences. Several researchers have reported studies for improvement of weld characteristics resulting from grain refinement occurring from grain size and grain structure. Controlling the input process parameters through optimization techniques to obtain good quality joints has thus attracted researchers to a greater extent. Design of experiments has been the most efficient, less time consuming and cost-effective way to predict the behaviour of the process parameters with minimum number of experiments. The multi-objective optimization techniques like TOPSIS and grey relational analysis are used to simultaneously optimize the process parameters and help acquire the desirable quality characteristics. The investigations on pulse current TIG welding has gained much concentration from researchers. Optimization of process parameters using TOPSIS has also been focused in the past where materials like Al6061 and Cu101 have been welded by micro friction stir welding for maximization of UTS, microhardness and minimization of surface roughness [3]. Hybrid optimization has been performed using NSGA-II and TOPSIS for friction stir welding of aluminium alloy 6061 series [4]. Welding of Inconel 625 was done by activated TIG welding process and optimum hardness and aspect ratio were determined by TOPSIS [5]. TOPSIS has also been used to optimize input process parameters during friction vibration welding of polypropylene glass composites [6]. Inconel 625 was welded by A-TIG process and optimization was performed using TOPSIS to obtain maximum depth of penetration, with increased microhardness, weld bead width and height in weld current [7]. The optimum condition for 316 Stainless Steel is welding current of 150 A, shielding gas flow rate of 15 l/min and weld speed of 190 mm/min that produce maximum UTS, impact strength and hardness obtained using Taguchi and GRA [8]. Ti-6Al-4V was welded by laser welding process and optimized by TOPSIS approach in order to maximize the hardness, depth of penetration and minimize the weld bead width [9]. Welding speed and shielding gas flow rate are two important weld parameters after laser power which influence the hardness and depth of penetration for joining hastelloy C-276 by laser welding and TOPSIS method is used to optimize the weld parameter [10]. Genetic Algorithm and PSO have been used to compare the predicted values obtained using design of experiments

[11]. Taguchi method has been employed for design and analysis of experimental results in pulse current tig welding process. Further, grey relational analysis has been performed to optimize multiple response factors simultaneously [12]. Authors have performed studies on optimization of process parameters to obtain sound weld characteristics and minimizing hardness in the weld zone in steels. During arc welding, continuous current flow produces high amount of heat leading to development of hot cracks, new phase formation, segregation of alloying elements [13-15]. Taguchi and TOPSIS have been combined in many recently conducted studies using electro-discharge machining [16], powder mixed electro discharge machining [17-19] and turning of steels where the input parameters have significant influence on the response factors [20-22]. The hybrid optimization techniques improve the performance characteristics and surface quality of the processes while establishing the optimal conditions for machining.

In the present work a five level four factor design technique has been used on experimental data for modeling of pulse current tig welding process. Process parameters selected for the test are peak current, base current, pulse frequency and shielding gas flow rate, considered in five different ranges, based upon the pilot experiment for the present investigation. Considering the number of input parameters and their levels,  $L_{25}$  orthogonal array has been used for the experiments. TOPSIS has been used to perform the optimization of process parameters and obtain the most suitable set of parametric combination to achieve maximized values of yield strength, ultimate tensile strength, flexural strength and microhardness. Microstructure analysis has been done for the optimal sample to evaluate the quality of the weld joint.

## 2. 2. Materials and Methods

### 2.1. Experimental Set up

The pulse tig welding set up used for the experiment is shown in Figure.1. The experiments were carried out with ER70S series filler wire. The chemical compositions of the base material, parent material and filler wire were measured using an X-Ray Fluorescence (XRF) analyser and is presented in Table 1. For shielding and back purging, commercial argon gas was employed. In welding equipment, automatic voltage regulation was offered. The influence of fixture variation has not been taken into account at the time of the trial. Both base plates were cleaned with acetone and a free cloth, and the grooved part was cleaned using a rotating stainless steel tool. Figure.2 shows the graphical illustration of the work process flow. For tensile testing, Instron UTM machine was used as shown in Figure.4 and Vickers's microhardness test was carried out for evaluating the hardness of the welded samples.



Figure 1. Pulse TIG Set up

2.2. Materials

SAILMA 450 and EN 14B steel were employed in this study, which are both commonly used for rear axle auto motive parts. SAILMA 450 is widely used for machine building, lifting equipment, architectural structures, containers, transport vehicle equipment, frame work structures, and bridge construction, and EN 14B steel is used for manufacturing machine tools, parts of the ship industry, vehicles, turbine fasteners, boiler support rods, gear shafts, valve and connecting rods, rotator blades, and excavator bucket teeth, among other applications. The joints of SAILMA 450 and EN 14B are used to make rear axles in automobile industries. Two foundation plates of

SAILMA 450 and EN 14B steel, with dimensions 60x60x5mm, were welded using pulse tig welding set up shown in Figure.1 with a square butt joint and a single 60v groove with suitable angle edge preparation. The samples prepared for tensile testing are shown in Figure.3. The mechanical properties of base and filler materials have been presented in Table 2. Figure.5 shows the tensile test samples after the test is performed.

Table 1. Chemical composition of base and filler material

Base metals/ Filler metals	C%	Mn%	S%	P%	Al%	Si%	Ni%	NB+Ti+V%
SAILMA 450	0.16	1.38	0.045	0.045	0.02	0.45	-	0.25
EN14 B	0.20	1.40	0.06	0.06	-	0.35	0.40	-
ER70S-6	0.15	1.40	0.035	0.02	-	0.80	0.15	0.03

Table 2 Mechanical properties of base and filler material

Base metals/ Filler metals	Yield strength (MPa)	UTS (MPa)	Hardness (Hv)	% Elongation
SAILMA 450	453	577	184	18
EN14 B	357	512	176	22
ER70S-6	452	538	167	22

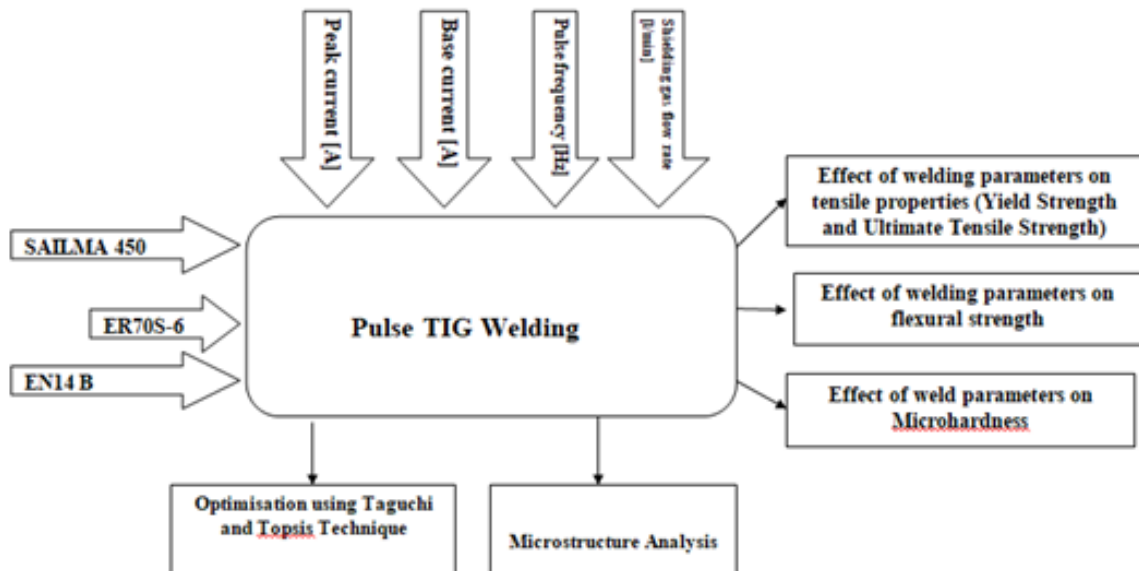


Figure 2. Graphical illustration of the work process of pulse current TIG welding of SAILMA 450 and EN-14B



Figure 3. Specimen preparation for tensile test



Figure 4. Instron UTM machine used for tensile test



Figure 5. Tensile specimen after testing

### 2.3. Design of experiments

Taguchi’s Technique is used to identify the influence of process parameters on the welding performance. The technique is simple and effective for quality optimization of processes and products. In the present study, the effect of pulse current tig welding process parameters has been investigated using Taguchi’s technique. Process parameters selected for the test are peak current, base current, pulse frequency and shielding gas flow rate in five different ranges, based upon the pilot experiment for the present investigation. Considering the number of input parameters and their levels, L<sub>25</sub> orthogonal array is used for the experiments as presented in Table 3. Taguchi’s process uses means to normalize the functions. Signal to noise (S/N) ratio reduces the variation in the output responses obtained from the experimental data by identifying the characteristic as “higher the better” (HB), Lower the better (LB) and nominal the best” (NB). The following equations are used to evaluate the type of performance characteristic using S/N ratio [23-24]. Table 4 shows the Taguchi’s L<sub>25</sub> orthogonal array used for the experiments along with the response values obtained in different runs.

Equation (1) and (2) represent the expressions for higher the better and lower the better used in Taguchi’s approach:

$$HB: S/N \text{ ratio} = -10 \log_{10} \left[ \frac{1}{n} \sum_{i=1}^n y_i^{-2} \right] \quad (1)$$

$$LB: S/N \text{ ratio} = -10 \log_{10} \left[ \frac{1}{n} \sum_{i=1}^n y_i^2 \right] \quad (2)$$

Table 3. Factors and their levels

Factors (Units)	Levels				
	Level 1	Level 2	Level 3	Level 4	Level 5
Peak current [A]	100	140	180	220	260
Base current [A]	60	80	100	120	140
Pulse frequency [Hz]	2	5	8	11	14
Shielding gas flow rate [l/min]	9	11	13	15	17

**Table 4.** L<sub>25</sub> experimental design with response variables

Run	I <sub>p</sub>	I <sub>b</sub>	F	Q	YS	UTS	FS	H
1	100	60	2	9	417	520	1163	174
2	100	80	5	11	420	529	1167	179
3	100	100	8	13	426	539	1170	182
4	100	120	11	15	429	540	1172	184
5	100	140	14	17	427	537	1171	181
6	140	60	5	13	423	532	1174	178
7	140	80	8	15	431	538	1182	183
8	140	100	11	17	434	541	1185	185
9	140	120	14	9	433	533	1177	182
10	140	140	2	11	430	531	1178	177
11	180	60	8	17	436	549	1188	189
12	180	80	11	9	440	548	1179	187
13	180	100	14	11	438	550	1176	191
14	180	120	2	13	435	547	1179	188
15	180	140	5	15	443	549	1186	194
16	220	60	11	11	439	556	1189	213
17	220	80	14	13	441	554	1191	211
18	220	100	2	15	442	550	1187	208
19	220	120	5	17	449	560	1199	218
20	220	140	8	9	452	557	1193	216
21	260	60	14	15	424	529	1166	177
22	260	80	2	17	426	531	1164	176
23	260	100	5	9	430	534	1159	178
24	260	120	8	11	432	536	1165	181
25	260	140	11	13	428	535	1167	180

2.4. Multi-objective optimization using Technique for order of preference by similarity to ideal solution (TOPSIS)

TOPSIS is a multi-criteria decision making technique which is used to find the best option from a set of alternatives. This approach is useful to convert multi-objective performance into a single objective performance as per desired condition by arranging all in ranking order. TOPSIS technique is widely used for decision making in manufacturing industries and among practitioners in cases where more number of alternatives and their interactions have significant impact on output responses. The approach is more efficient and easy to use. The chosen criteria must be close to the positive best solution and far away from the negative best solution, making the relative closer to the ideal solution as the best solution. The steps followed are expressed as:

Step-1: In first step of TOPSIS method, decision matrix is formed which having ‘r’ attributes and ‘c’ alternatives which can be expressed as:

$$D_m = \begin{bmatrix} k_{11} & k_{12} & k_{13} & \dots & \dots & k_{1r} \\ k_{21} & k_{22} & k_{23} & \dots & \dots & k_{2r} \\ k_{31} & k_{32} & k_{33} & \dots & \dots & k_{3r} \\ \vdots & \vdots & \vdots & \ddots & \ddots & \vdots \\ \vdots & \vdots & \vdots & \ddots & \ddots & \vdots \\ k_{c1} & k_{c2} & k_{c3} & \dots & \dots & k_{cr} \end{bmatrix} \quad (3)$$

Where, K<sub>lm</sub> is represented as performance of l<sup>th</sup> alternative for m<sup>th</sup> attribute.

Step 2: Now normalized matrix has to be obtained by using the given formula:

$$J_{lm} = \frac{k_{lm}}{\sqrt{\sum_{i=1}^c k_{im}^2}} \quad \text{where } m=1, 2, 3, \dots, r \quad (4)$$

Step-3: Each attributes weight was assumed as W<sub>m</sub> (m=1,2,3,...r). The weighted normalized decision matrix F= [ v<sub>lm</sub>] can be obtained by using:

$$F = W_m J_{lm} \quad (5)$$

Where  $\sum_{m=1}^r W_m = 1$

Step 4: The positive and negative ideal solutions can be calculated by using the expressions given by:

$$F^+ = \left\{ \left( \sum_l^{\max} f_{lm} \mid m \in M \right), \left( \sum_l^{\min} m \mid m \mid l = 1, 2, \dots, c \right) \right\} \\ = \{f^+_{1}, f^+_{2}, f^+_{3}, \dots, f^+_{r}\} \quad (6)$$

$$F^- = \left\{ \left( \sum_l^{\min} f_{lm} \mid m \in M \right), \left( \sum_l^{\max} m \mid m \mid l = 1, 2, \dots, c \right) \right\} \\ = \{f^-_{1}, f^-_{2}, f^-_{3}, \dots, f^-_{r}\} \quad (7)$$

Step 5: Separation between alternatives was calculated. Separation of each alternative from ideal solution is expressed as:

$$S_i^+ = \sqrt{\sum_{m=1}^r (f_{lm} - f_m^+)^2}, \quad l=1, 2, \dots, c \quad (8)$$

And separation of each alternative from negative ideal solution is given as:

$$S_i^- = \sqrt{\sum_{m=1}^r (f_{lm} - f_m^-)^2}, \quad l=1, 2, \dots, c \quad (9)$$

Step 6: The relative closeness of an alternative to the ideal solution can be expressed as:

$$P_i = \frac{S_i^-}{S_i^+ + S_i^-} \quad \text{where } l=1, 2, 3, \dots, c \quad (10)$$

Step 7: The P<sub>i</sub> value is ranked in descending order to get the alternatives with best and worst solutions.

3. Results and discussion

3.1. Effect of welding parameters on tensile properties

Weld quality and weld life depend upon the weldability of base materials. The weld life is dependent on the mechanical behaviour of the welded joint which is governed by the microstructural changes taking place within the work material. For any arc welding process, welding current plays a vital role for melting of base material. Choosing the appropriate range of welding current depends on the base material thermal properties and material thickness [11]. Determining the proper range of welding current particularly for pulse TIG welding is a challenging task as it involves the action of two currents viz. peak current and base current. Generally, base current is chosen in such a way that roots mean square of current value becomes 70% of peak current value. Peak current helps to melt the base material, so heat input and depth of penetration are mainly influenced by the value of peak current which has direct impact on mechanical properties and in microstructural changes. It has been observed by the experimental results that as the peak current range increases, the yield strength and ultimate tensile strength

also increase. This is due to the increase in heat input in the weld zone which improves the weld depth of penetration. The maximum yield strength and UTS are achieved at a peak current of 220 A as shown in Figure.6 (a) and (b). Beyond 220A of peak current with combination of other input parameters, the mechanical strength gets reduced due to the high current input which produces defects like undercut and coarser grain in weld zone. For a peak current of 100 A, the yield strength is about 422 MPa and UTS achieved is 536 MPa which is lower than other peak current values due to lack of fusion. Thus low peak current value is not sufficient to melt the base metal completely but with rise in peak current from 100 A to 220 A, yield strength and ultimate tensile strength increase with suitable combination of other welding process parameters like base current, pulse frequency and shielding gas flow rate as shown in

Figure.6(c), (d), (e), (f), (g), (h). At a peak current of 180 A, low pulse frequency and high shielding gas flow rate, the yield strength gets reduced. It may be due to less pulse frequency which is not able to produce stable arc and is associated with defects like porosity caused by high shielding gas flow rate. At a peak current of 140 A, with very low base current and low pulse frequency, tensile strength gets reduced as the welding current is not sufficient to melt the base material as well as for maintaining the weld arc. Hence, optimized welding parameters are preferable for achieving better mechanical properties for welded joints and suitable joint strength. Maximum YS is achieved at an  $I_b$  of 140 A and maximum UTS is observed at an  $I_b$  of 110A. The variation of yield strength and UTS with the chosen input parameters is shown in Figure. 6(a)-Figure. 6(h).

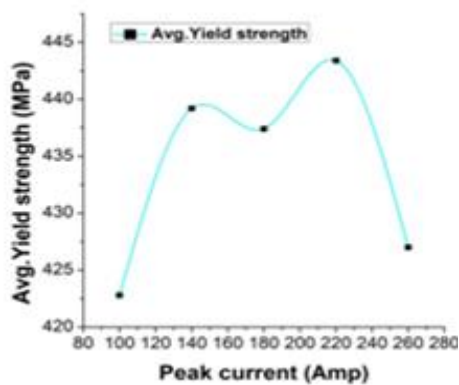


Figure 6. (a) Variation of Yield Strength with  $I_p$

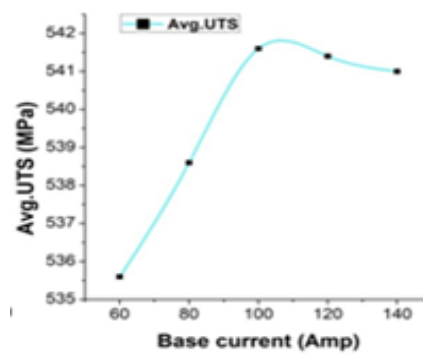


Figure 6. (d) Variation of UTS with  $I_b$

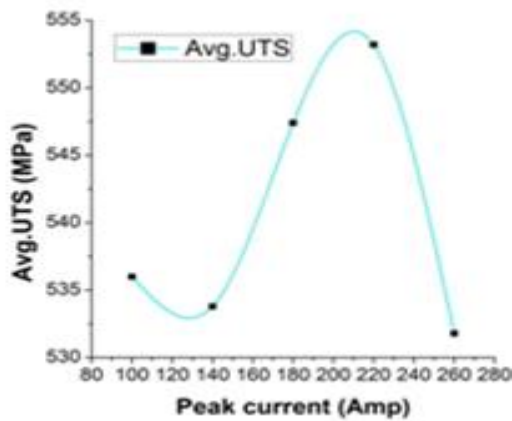


Figure 6. (b) Variation of UTS with  $I_p$

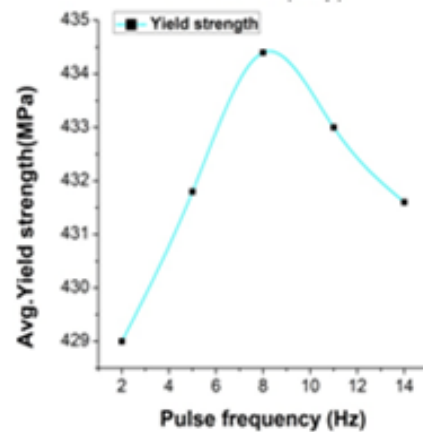


Figure 6. (e) Variation of Yield Strength with PF

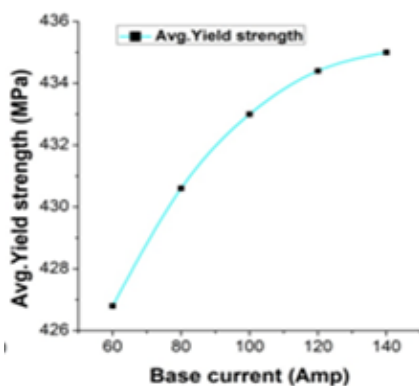


Figure 6. Variation of Yield Strength with  $I_b$

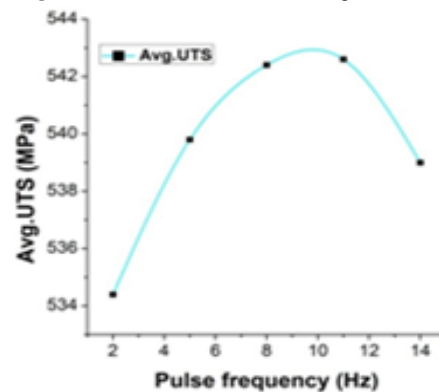


Figure 6. (f) Variation of UTS with PF

3.2. Effect of welding parameters on flexural strength

To predict formation of a sound weld joint and susceptibility to crack formation in the weld zone, flexural strength test is performed. To find out the flexural strength, a three point bending test is done for all the welded samples. Maximum flexural strength of around 1190 MPa is found for a peak current of 220 A with high shielding gas flow rate. Flexural strength is mainly influenced by high temperature produced by increased welding current range along with high shielding gas flow rate. Base current and pulse frequency have less significance on bonding strength than comparatively peak current and shielding gas flow rate. By using the argon shielding gas and high peak current, the bonding strength in fusion zone gets increased due to high heat input which causes rise in welding temperature, leading to more solidification time and change in microstructure. In fusion zone microstructure change takes place by grain refinement which forms smaller nuclei and improves the bonding strength. It is observed that for a base current of 100 A with lowest and highest range value of peak current flexural strength drastically decrease which may be attributed to the low depth of penetration which involves more solidification time in weld pool and produces coarser grains and result in formation of welding defects like undercut and shrinkage. Lower value of argon shielding gas flow rate with lowest pulse frequency range chosen also minimizes the flexural strength due to low temperature in weld pool. Figure. 7 (a), (b), (c), (d) show the variation of flexural strength with the selected input parameters.

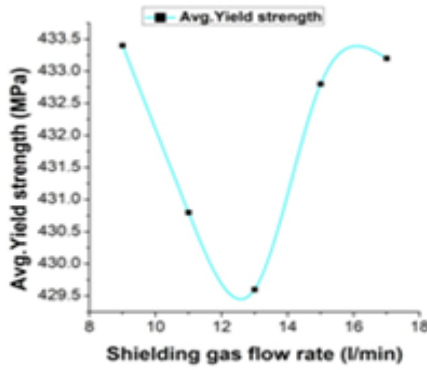


Figure 6. (g) Variation of YS with Q

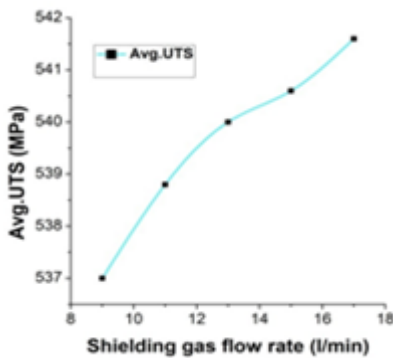


Figure 6. (h) Variation of UTS with Q

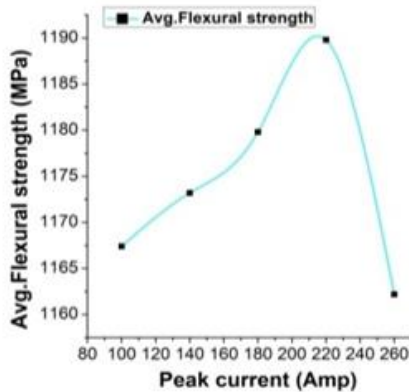


Figure 7. (a) Variation of FS with  $I_p$

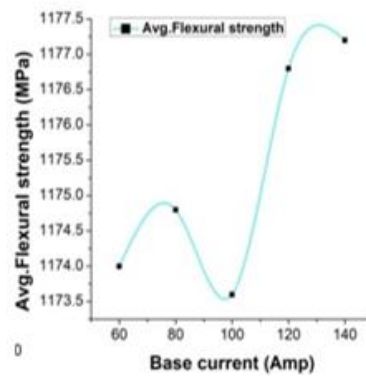


Figure 7. (b) Variation of FS with  $I_b$

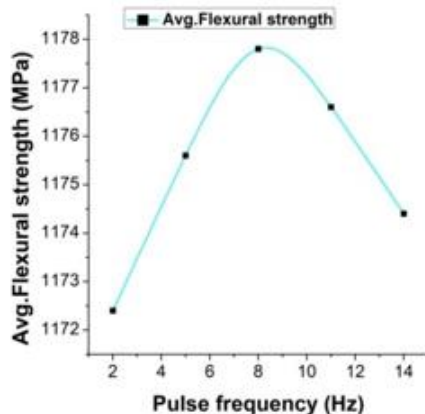


Figure 7. (c) Variation of FS with PF

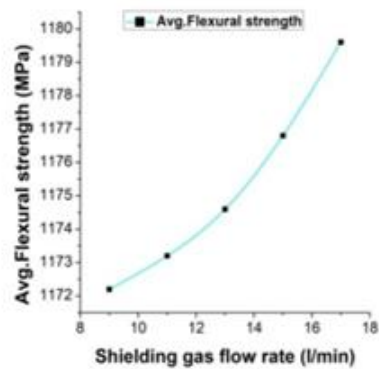


Figure 7. (d) Variation of FS with Q

3.3. Effect of weld parameters on microhardness

To predict the resistance to deformation in the welded joints, microhardness test is performed at different points in the welded zone and nearby heat affected regions with a diamond indenter. The resultant indentation is measured with the help of an optical microscope. The microhardness value increases with the increase in peak current and pulse frequency. In fusion zone, grain refinement is mostly influenced by pulse frequency. Optimum pulse frequency produces finer grain and choosing higher pulse frequency with high input or high peak current results in formation of coarser grains. This is due to the requirement of sufficient and longer cooling times in the absence of which coarser grains are formed which consequently result in lower hardness values. Increase in peak current upto 220 A with optimum range of other weld input parameters leads to increase in hardness value. Beyond 220 A current, the microhardness value decreases with any combination of

input process parameters. Lowest hardness value is recorded for shielding gas flow rate 13 l/min with low base current and lowest and highest value of pulse frequency. This decrease in microhardness is due to welding defects like porosity, unstable arc formation and wider weld bead width. Apart from these factors microhardness value gets varied with respect to temperature generated by interpass weld and thickness of plate. Figure.8 (a), (b), (c) (d) show the variation of microhardness with other input parameters.

3.4. ANOVA analysis

3.4.1. ANOVA for Yield Strength

The significant process parameters affecting yield strength can be determined using analysis of variance (ANOVA) [25]. ANOVA result for means of YS is given in Table 5 which indicates that the  $I_p$ ,  $I_b$  and  $F$  are parameters which have significant contribution towards improvement in YS while the role of  $Q$  is insignificant.

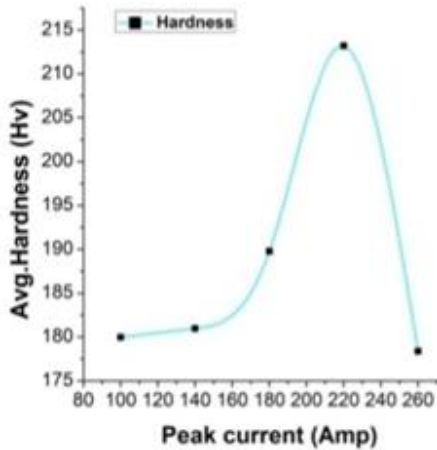


Figure 8. (a) Variation of microhardness with  $I_p$

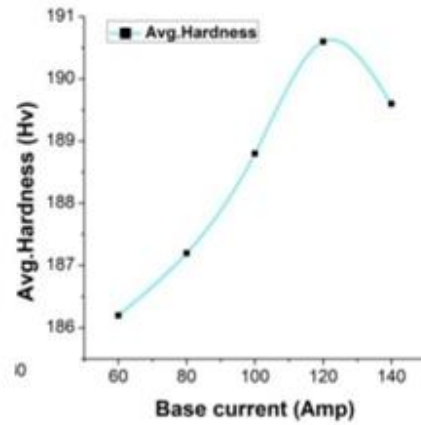


Figure 8. (b) Variation of microhardness with  $I_b$

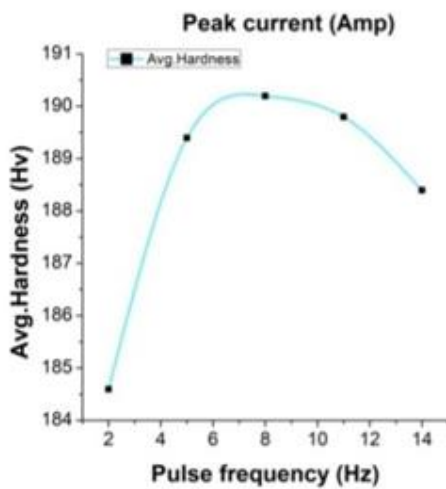


Figure 8. (c) Variation of microhardness with PF

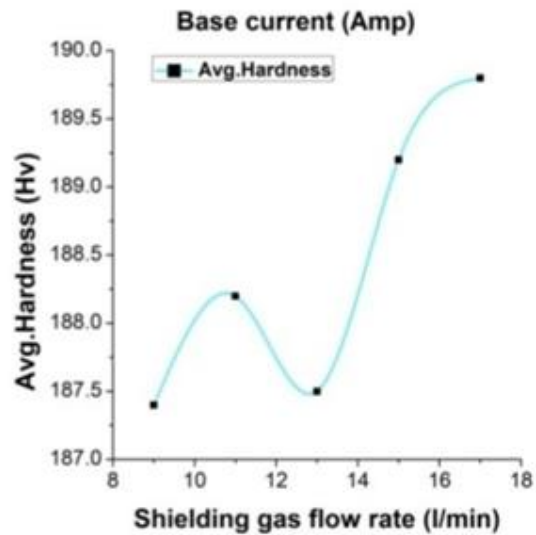


Figure 8. (d) Variation of microhardness with  $Q$

**Table 5.** ANOVA table for means of YS

Source	DF	Adj SS	Adj MS	F	P
I <sub>p</sub>	4	1990.16	497.54	89.81	0.000
I <sub>b</sub>	4	130.96	32.74	5.91	0.016
F	4	221.36	55.34	9.99	0.003
Q	4	66.96	16.74	3.02	0.086
Residual Error	8	44.32	5.54		
Total	24	2453.76			
S= 2.35372	R- Sq=98.19%	R- Sq(adj)=94.58%			

**3.4.2. ANOVA for Flexural Strength**

The significant process parameters affecting flexural strength using ANOVA analysis has been presented in Table 7 which indicates that the I<sub>p</sub> and Q are parameters which have significant contribution towards improvement in FS while the role of I<sub>b</sub> and F is insignificant.

**Table 7.** ANOVA table for means of FS

Source	DF	Adj SS	Adj MS	F	P
I <sub>p</sub>	4	2340.64	585.16	95.77	0.000
I <sub>b</sub>	4	53.44	13.36	2.19	0.161
F	4	85.84	21.46	3.51	0.061
Q	4	176.24	44.060	7.21	0.009
Residual Error	8	48.88	6.110		
Total	24	2705.04			
S= 1.4282	R- Sq=99.19%	R- Sq(adj)=94.58%			

**3.4.3. ANOVA for microhardness**

The significant process parameters affecting yield strength can be determined using analysis of variance (ANOVA). ANOVA result for means of YS is given in Table 8 which indicates that the I<sub>p</sub>, I<sub>b</sub> and F are parameters which have significant contribution towards improvement in YS while the role of Q is insignificant.

**Table 8.** ANOVA table for means of YS

Source	DF	Adj SS	Adj MS	F	P
I <sub>p</sub>	4	4211.44	1052.86	295.75	0.000
I <sub>b</sub>	4	63.44	15.86	4.46	0.035
F	4	103.04	27.76	7.24	0.009
Q	4	19.84	4.96	1.39	0.319
Residual Error	8	28.48	3.56		
Total	24	4426.24			
S= 1.8868	R- Sq=99.36%	R- Sq(adj)=98.07%			

**3.5. TOPSIS**

Optimum range of welding process parameters are found out for output responses like Yield strength, Ultimate tensile strength, flexural strength and

microhardness using TOPSIS. The preference value for each experimental combination can be achieved using equation (4-9) considering that the preference value has comparative nearness to the best solution. The normalized matrix is shown in Table 9. The ratio of negative ideal separation measure divided by the sum of negative ideal separation measure and the positive ideal separation measure gives the best solution and is calculated using equation (10). Equal weightage is assigned considering the performance parameters equally important while welded under ideal conditions. The weighted normalized matrix is shown in Table 10. A multi-attribute optimization problem is transformed into single objective optimization problem using a Taguchi based TOPSIS approach. Table 11 shows the preference values of TOPSIS for each run. The experimental run with maximum preference value and highest rank has relative closeness to the ideal solution and is considered as best value. It is apparent that run 19 achieves highest preference order with multiple performance characteristics and is thus the optimal set of process parameters followed by run 20 and run 16. The optimal setting obtained is I<sub>p</sub>4I<sub>b</sub>4F<sub>2</sub>Q<sub>5</sub>.

**Table 9.** Normalized Matrix

Run	YS	UTS	FS	H
1	0.193	0.1923	0.1975	0.1841
2	0.194	0.1956	0.1984	0.1894
3	0.197	0.1993	0.1989	0.1926
4	0.198	0.1997	0.1992	0.1947
5	0.197	0.1986	0.199	0.1915
6	0.195	0.1967	0.1994	0.1884
7	0.199	0.1989	0.2007	0.1937
8	0.2004	0.2001	0.2013	0.195
9	0.1999	0.1971	0.1999	0.1926
10	0.1985	0.196	0.2001	0.1873
11	0.201	0.2026	0.2018	0.20005
12	0.2032	0.2023	0.2002	0.1979
13	0.2022	0.2030	0.1997	0.2021
14	0.2009	0.2019	0.2004	0.1989
15	0.204	0.2041	0.2014	0.2053
16	0.2027	0.2052	0.2019	0.2254
17	0.2036	0.2045	0.2023	0.2233
18	0.2041	0.2034	0.2016	0.2201
19	0.2069	0.206	0.2036	0.2307
20	0.2087	0.2056	0.2026	0.2286
21	0.1958	0.1952	0.198	0.1873
22	0.1967	0.1963	0.1977	0.1862
23	0.1985	0.1975	0.1968	0.1884
24	0.1995	0.1982	0.1979	0.1915
25	0.197666	0.1978	0.1982	0.1905

### 3.5.1. Confirmatory experiment for TOPSIS

After getting optimized parameter setting, for improving the quality characteristic, prediction and confirmation test is carried out for optimal set of process parameters. An increase in yield strength, UTS, flexural strength and microhardness values are obtained for optimized parameter setting and are presented in Table 12. The improvement in preference value for ideal solution is 0.5457.

**Table 10.** Weighted normalized matrix with positive and negative ideal solutions

Run	WYS	WUTS	WFS	WH	$S_i^+$	$S_i^-$
1	0.04814	0.048	0.0493	0.046044	0.012887	0.000171
2	0.04849	0.0489	0.0496	0.047367	0.011345	0.001647
3	0.04918	0.049	0.0497	0.048161	0.010199	0.002987
4	0.04953	0.0499	0.0498	0.04869	0.009578	0.003566
5	0.0493	0.0496	0.0497	0.047897	0.01044	0.002749
6	0.04883	0.0491	0.0498	0.047103	0.011393	0.001801
7	0.04976	0.0497	0.0501	0.048426	0.009763	0.003469
8	0.05011	0.05002	0.05032	0.048955	0.009119	0.004165
9	0.04999	0.0492	0.049986	0.048161	0.01007	0.003154
10	0.04964	0.049	0.050029	0.046838	0.011457	0.002099
11	0.05034	0.0506	0.050454	0.050013	0.007952	0.00537
12	0.0508	0.0505	0.050071	0.049484	0.008415	0.005089
13	0.05057	0.0507	0.049944	0.050543	0.007429	0.005821
14	0.05022	0.0504	0.050114	0.049749	0.008282	0.004966
15	0.05115	0.051	0.050369	0.051337	0.006477	0.006868
16	0.0506	0.0513	0.050497	0.056364	0.002057	0.011186
17	0.05092	0.0511	0.050582	0.055835	0.002304	0.010713
18	0.05103	0.0508	0.050412	0.055041	0.003004	0.009923
19	0.05173	0.0515	0.050922	0.057688	0.000463	0.01277
20	0.05219	0.0514	0.050667	0.057158	0.000595	0.012375
21	0.04895	0.0488	0.049518	0.046838	0.011722	0.001387
22	0.04918	0.04909	0.049433	0.046573	0.011858	0.001564
23	0.04964	0.04937	0.04922	0.047103	0.011223	0.00225
24	0.04987	0.04956	0.049476	0.047897	0.010349	0.00295
25	0.049417	0.04946	0.049561	0.047632	0.010717	0.002487

**Table 11** Preference values with rank order

Run	Preference value	Rank
1	0.013062	25
2	0.126773	22
3	0.226548	15
4	0.2713	12
5	0.208409	17
6	0.136519	21
7	0.262164	13
8	0.313552	11
9	0.238477	14
10	0.154813	20
11	0.403088	8
12	0.376845	9
13	0.43932	7
14	0.374851	10
15	0.514665	6
16	0.844689	3
17	0.823034	4
18	0.767603	5
19	0.965024	1
20	0.954109	2
21	0.105796	24
22	0.116547	23
23	0.167011	19
24	0.221839	16
25	0.188375	18

**Table 12.** Results of confirmatory experiment

Initial factor setting	Optimal set	
	Initial	Experimental
Level	$I_{p3}I_{b3}F_3Q_3$	$I_{p4}I_{b4}F_2Q_5$
Peak current	180	220
Base current	100	120
Pulse frequency	8	5
Shielding gas flow rate	13	17
Value of preferred solution	0.4193	0.965024

3.5.2. ANOVA for TOPSIS

ANOVA is useful to determine the effect of input process parameters on output responses. Table.13 shows the ANOVA results for preference solution. Using MINITAB software, the result of factor responses were considered following “higher the better” criterion. From the response table of means shown in Table 14, it is clear that peak current, pulse frequency and base current have more contribution for improvement in the value of preference solution than the shielding gas flow rate. Figure.9 shows the variation of S/N ratio for the preference value. From the S/N ratio it can be observed that the trend of variation of all the process parameters is initially increasing followed by a decrease. This shows that as the current and pulse frequency increase, the weld quality shows deterioration. The most optimum setting is at the moderate values of all parameters [17-18].

Table 13. ANOVA table for TOPSIS

Source	DF	Adj SS	Adj MS	F-value	P-value
Peak current	4	1.80079	0.450198	352.45	0.000
Base current	4	0.04466	0.011166	8.74	0.005
Pulse frequency	4	0.05039	0.012598	9.86	0.003
Shielding gas flow rate	4	0.01069	0.002674	2.09	0.174
Error	8	0.01022	0.001277		
Total	24	1.91676			

Table 14. Response table for means of preference value

Factor	Response for means of preference value						
	Level-1	Level-2	Level-3	Level-4	Level-5	Delta	Rank
Peak current	0.1692	0.2211	0.4217	0.8708	0.1599	0.7109	1
Base current	0.3006	0.3410	0.3828	0.4142	0.4040	0.1136	3
Pulse frequency	0.2853	0.3819	0.4135	0.3989	0.3630	0.1281	2
Shielding gas flow rate	0.3499	0.3574	0.3498	0.3843	0.4013	0.0514	4

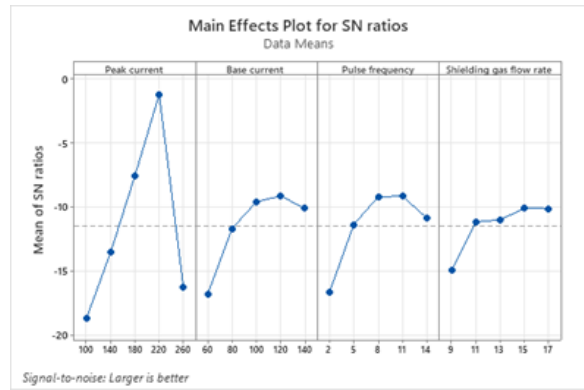
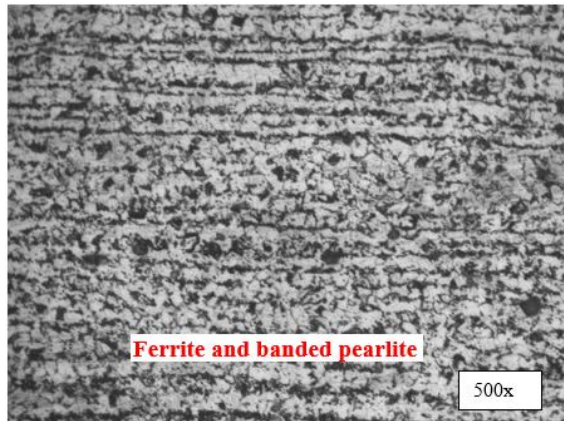


Figure 9. S/N ratio plot for preference value

4. Microstructure analysis

Microstructure analysis has been carried out for the base material, heat affected zone and fusion zone for optimized weld samples at 500x magnification. Figure.10 (a),(b),(c) and Figure.11(a),(b),(c) represent the base material microstructure, microstructures at HAZ and fusion zone for SAILMA 450 and EN 14B respectively. From the microstructure shown in Figure. 10(a), it can be observed that for SAILMA 450, the base structure is mostly ferrite and pearlite is present in banded form. Fine equiaxed grains are observed which are mixture of ferrite and pearlite. The presence of pearlite helps to retain the strength of the material. Since the material possess more strength, it is used in power plants and finds application as a construction material. Figure. 10(b) shows the microstructure at the heat affected zone (HAZ) at SAILMA450 side. The HAZ involves the presence of EN-14B due to fusion, hence demonstrates change in structure and properties. Pearlite transforms into bainitic structure. The microstructure thus contains bainite, pearlite and ferrite. Figure. 10(c) shows a fused structure combining bainite, pearlite and ferrite. In EN 14B, the base material consists of lower pearlite with some ferrite present in it. The grains are equiaxed and finer in nature as observed in Figure. 11(a).The microstructure at heat affected zone of EN-14B shown in Figure. 11(b)consists of bainite.The grains appear to be coarser which improve the creep properties of the material. In the fusion zone, transformation occurs from bainite to lower martensite with reduced grain size as shown in Figure 11(c). The microstructure contains pearlite, ferrite, tempered martensite and the weld zone shows good compatibility.



**Figure 10.** (a) Base Material microstructure of SAILMA 450 captured at 500x

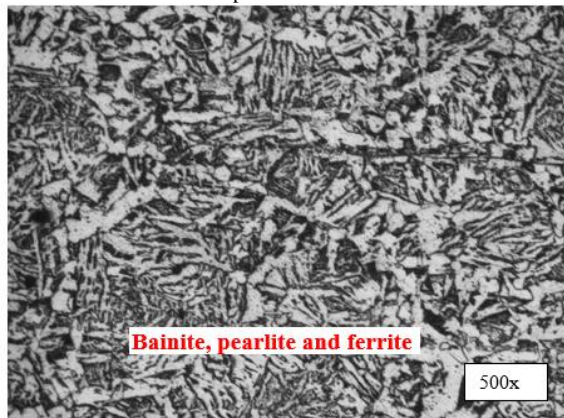


**Figure 10.** (b) Grain orientation at HAZ captured at 500x

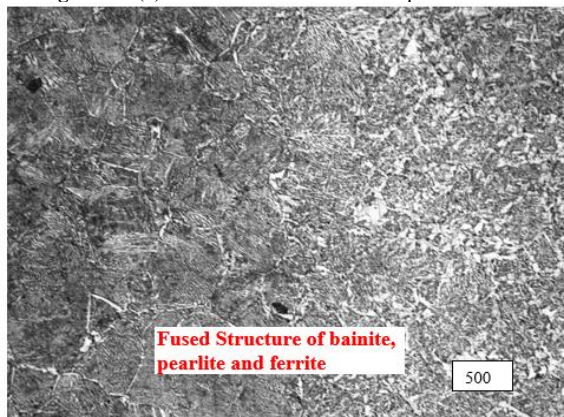


**Figure 10.** (c) Microstructure at fusion zone for SAILMA 450 captured at 500x

## 5. Conclusion

The present study involves pulse current tig welding of SAILMA 450 with EN 14B steel. The process parameters have been optimized using Taguchi technique and multi-objective optimization has been performed using TOPSIS to maximize yield strength, ultimate tensile strength, flexural strength and microhardness simultaneously. The major conclusions drawn are as follows:

1. Pulse current TIG welding process is considered to be among the most difficult welding processes used in industries. The process is slower, involves complexity and is difficult to master. It requires high skill of

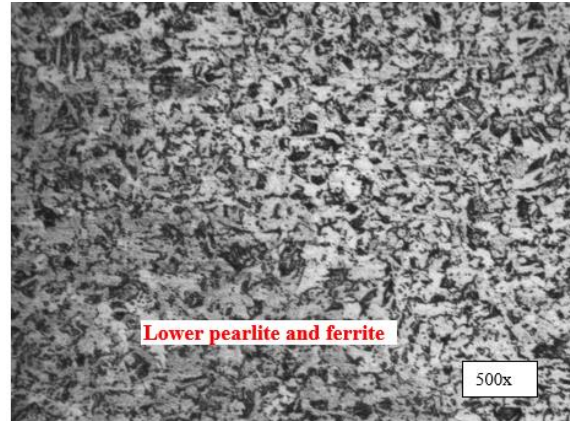


**Figure 11.** (a) Base Material microstructure captured at 500x

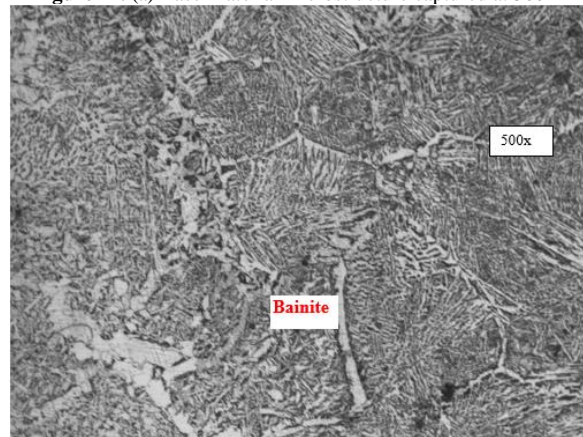


**Figure 11.** (b) Grain orientation at HAZ captured at 500x

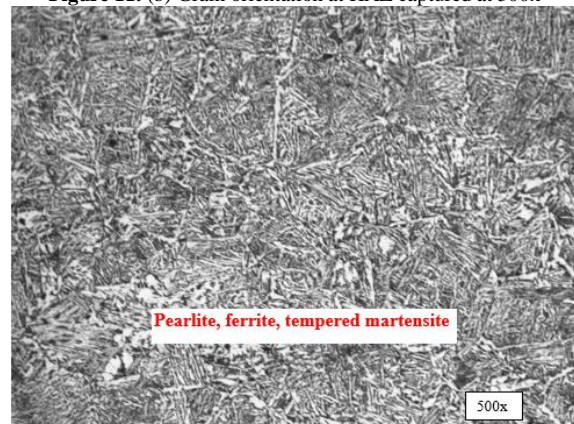


**Figure 11.** (c) Microstructure at fusion zone for EN 14B captured at 500x

operation, greater care and the welder must maintain a short arc length to prevent contact between electrode and workpiece.

2. Design of experiments has been used to establish the relationship between process variables. TOPSIS has been used to optimize the process parameters simultaneously to achieve maximized output in terms of mechanical strength and hardness of the weld joint.
3. The optimum set of process parameters for achieving maximized mechanical strength and microhardness is peak current of 220 A, base current of 120 A, pulse frequency of 5 Hz and shielding gas flow rate 17 l/min.
4. Yield strength and ultimate tensile strength increase with increase of current but when pulse frequency is

- beyond 8Hz then the mechanical strength gets reduced due to arc instability produced by high pulse frequency.
5. For flexural strength, peak current and shielding gas flow rate are more dominant parameters than base current and pulse frequency.
  6. Microhardness value increases up to a peak current of 220 A with pulse frequency of 5Hz and after that the microhardness value gets reduced due to grain coarsening.
  7. The tensile specimen usually fails at the base metal side of EN 14B steel due to less tensile strength than SAILMA 450 steel side.
  8. No crack has been found up to 120° of three point bending test which proves that welded joints are more ductile in nature.
  9. Microstructure of weld zone consists of martensitic structure which leads to increase in the hardness. Finer grains are observed in SAILMA 450 fusion zone side than fusion zone side of EN 14B.
  10. TOPSIS acts as a powerful tool for optimization of the process. Confirmatory tests show an improvement of 0.5457 in the preference values which is acceptable. The achieved results show that the optimized set of process parameters may be used in the industries to achieve good quality welded structures during welding of SAILMA 450 and EN14B. These steels have been combined together for various applications and have been welded by advanced welding processes like friction stir welding.
  11. The suggested work can be extended further and brought to application in automotive industries. Also, the optimization methods may be used to solve problems in other manufacturing processes like conventional and non-conventional machining, forming etc.

## References

- [1] L. Liu, X. Xu, G. Xu, G., Z. Zhang, "Effect of laser on double-arc physical characteristics in pulsed laser induced double-TIG welding". *International Journal of Advanced Manufacturing Technology*, Vol.119 (2021), 1515-1529.
- [2] T.S. Balasubramanian, M. Balakrishnan, V. Balasubramanian, M.M. Manickam, "Influence of welding processes on microstructure, tensile and impact properties of Ti-6Al-4V alloy joints". *Transactions of Nonferrous Metals Society of China*, Vol. 21 (2011) No. 6, 1253-1262.
- [3] M.S. Manohar, K. Mahadevan, "Multi-response optimization of weld-process variables for micro-friction stir welding of Al6061 (T6) and Cu101 sheets using Topsis Method". *IOP Conf. Series: Materials Science and Engineering*, Vol. 1168 (2021) No. 012002.
- [4] T. Medhi, S.A.I. Hussain, B.S. Roy, S.C. Saha, "An Intelligent Multi-Objective framework for optimizing friction-stir welding process parameters". *Applied Soft Computing*, Vol.104 (2021) No.107190.
- [5] J. Sivakumar, N.N. Korra, "Optimization of welding process parameters for activated tungsten inert welding of Inconel 625 using the technique for order preference by similarity to ideal solution methodology." *Arabian Journal for Science and Engineering*, Vol.46 (2021), 7399-7409.
- [6] D.J. Daniel, K. Panneerselvam, "Process parameters optimization for friction vibration joining of polypropylene/spherical glass composites using Topsis." *Surface Review and letters*, Vol. 27 (2020) No.06, 1950167.
- [7] J. Sivakumar, M. Vasudevan, M., N.N. Korra, "Systematic welding process parameter optimization in activated tungsten inert gas (A-Tig) welding of Inconel 625." *Transactions of the Indian Institute of Metals*, Vol. 73(2020) No.3, 555-569.
- [8] V. Chodha, R. Dubey, R. Kumar, S. Singh, S. Kaur, "Selection Of Industrial Arc Welding Robot With Topsis And Entropy Mcdm Techniques." *Material Today Proceedings*, Vol. 50 (2022) No. 5, 709-715.
- [9] K. R. Sampreet, V. Mahidhar, R. Kannan, T. D. B. Kannan, "Optimization of Parameters In Nd: Yag Laser Welding of Ti-6Al-4V using Topsis." *Material Today Proceedings*, Vol. 21 (2020), 244-247.
- [10] V. Mahidhar, K.R. Sampreet, R. Kannan, T. D. B. Kannan, "Parameter optimization in laser welding of hastelloy C-276 using Topsis." *Material Today Proceeding*, Vol.21 (2020) 595-600.
- [11] P.K. Baghel, T. Gupta, "Optimization of parameters of pulse current gas tungsten arc welding using non conventional techniques". *Journal of advanced joining processes*, Vol.6 (2022) No. 100124.
- [12] S. Avinash, Y. Balram, B. S. Babu, G. Venkatramana, "Multi-response optimization of pulse TIG welding process parameters of welds AISI 304 and Monel 400 using grey relational analysis". *Material Today Proceedings*, Vol. 19 (2019) No.2, 296-301.
- [13] A.K.Srirangan, P. Sathiyar, "Optimisation of Process Parameters for Gas Tungsten Arc Welding of Incoloy 800HT Using TOPSIS". *Materials Today: Proceedings*, Vol. 4 (2017) No.2, 2031-2039.
- [14] J. Joseph, S. Muthukumar, "Optimization of activated TIG welding parameters for improving weld joint strength of AISI 4135 PM steel by genetic algorithm and simulated annealing." *International Journal of Advanced Manufacturing Technology*, Vol.93 (2017), 23-34
- [15] G. Magudeeswaran, S.R. Nair, L. Sundar, N. Harikannan, "Optimization of process parameters of the activated tungsten inert gas welding for aspect ratio of UNS S32205 duplex stainless steel welds." *Defence Technology*, Vol. 10 (2014) 251-260.
- [16] H.P.Nyugen, V.D.Phm, N.V.Ngo. "Application of TOPSIS to Taguchi method for multi-characteristic optimization of electrical discharge machining with titanium powder mixed into dielectric fluid." *International Journal of advanced manufacturing Technology*, Vol. 98 (2018), 1179-1198.
- [17] Tripathy, S., Tripathy, D.K.: Multi-attribute optimization of machining process parameters in Powder Mixed Electro-Discharge Machining using TOPSIS and Grey Relational Analysis. *Engineering Science and Technology: An International Journal*, 19(1), 62-70 (2016).
- [18] Tripathy, S. and Tripathy, D.K. 'Multi-response optimization of machining process parameters for powder mixed electro-discharge machining using grey relational analysis and topsis.' *Machining Science and Technology*, Vol. 21(3), (2017); p.362-384.
- [19] G.Talla, D. K. Sahoo, S. Gangopadhyay, C.K. Biswas, "Modeling and multi-objective optimization of powder mixed electric discharge machining process of aluminium /alumina metal matrix composite." *Engineering Science and Technology: an International Journal*, pp. 1-5, (2015).
- [20] S. Balasubramanian, T. Selvaraj, "Application of integrated Taguchi and TOPSIS method for optimization of process parameters for dimensional accuracy in turning of EN25 steel." *Journal of the Chinese Institute of Engineers*, Vol.40 (2017) No. 4, 267-274.
- [21] A.Singh, S.Datta, S.S.Mahapatra, "Application of TOPSIS in the Taguchi Method for optimal machining parameter

- selection. "Journal for Manufacturing Science and production, Vol.11(2011) No. 1-3, 49-60.
- [22] B.Singaravel, T.Selvaraj, " Application of Taguchi method for optimization of parameters in turning operation." Journal for Manufacturing Science and production, Vol.16(2016) No.3, 183-187.
- [23] M. Soori , M. Asmael, "A Review of the Recent Development in Machining Parameter Optimization."Jordan Journal of Mechanical and Industrial Engineering, Vol.16 (2022) No.2, 205-223.
- [24] H. Q. Ayun, J. Triyono, E. Pujiyanto, "Optimization of Injection Molding Simulation of Bioabsorbable Bone Screw Using Taguchi Method and Particle Swarm Optimization." Jordan Journal of Mechanical and Industrial Engineering, Vol.16 (2022) No.2, 319-325.
- [25] G.V.S.S.Sharma, P. Srinivasa Rao , B. Surendra Babu, "Establishing Process Capability Indices in a Sugar Manufacturing Industry – an Industrial Engineering Perspective." Jordan Journal of Mechanical and Industrial Engineering, Vol.15 (2021) No.4, 319-325.